Superconductor Science and Technology

PAPER

Size evolution of the oxygen interstitial nanowires in La_2CuO_{4+y} by thermal treatments and x-ray continuous illumination

To cite this article: Nicola Poccia *et al* 2012 *Supercond. Sci. Technol.* **25** 124004

Supercond. Sci. Technol. **25** (2012) 124004 (6pp) doi:10.1088/0953-2048/25/12/124004

Size evolution of the oxygen interstitial nanowires in La_2CuO_{4+y} by thermal treatments and x-ray continuous illumination

Nicola Poccia[1,2], Antonio Bianconi[2,3,4], Gaetano Campi[5], Michela Fratini[6] and Alessandro Ricci[7]

[1] European Synchrotron Radiation Facility, B.P. 220, F-38043 Grenoble Cedex, France
[2] Department of Physics, Sapienza University of Rome, Piazzale Aldo Moro 2, I-00185 Roma, Italy
[3] Rome International Center of Materials Science, Superstripes, (RICMASS) via dei Sabelli 119A, I-00185 Roma, Italy
[4] Mediterranean Institute of Fundamental Physics, (MIFP) Marino, Italy
[5] Institute of Crystallography, CNR, Via Salaria Km 29.300, Monterotondo Stazione, Roma, I-00015, Italy
[6] Fermi Center, Piazzale del Viminale, I-00187 Roma, Italy
[7] Deutsches Elektronen-Synchrotron DESY, Notkestraße 85, D-22607 Hamburg, Germany

E-mail: Nicola Poccia@roma1.infn.it

Received 30 May 2012, in final form 24 July 2012
Published 8 November 2012
Online at stacks.iop.org/SUST/25/124004

Abstract
Using synchrotron x-ray diffraction as pump and probe, we show how the oxygen interstitials (Oi) become ordered as a function of temperature under x-ray continuous illumination in an optimum doped La_2CuO_{4+y} superconductor. The evolution of Oi grain size and phase segregation is shown by thermal treatments, providing a new experimental avenue for tuning quantum size effects in the system through the direct control of the size of the Oi grains. Here we report the ordering of oxygen interstitials, cooling the sample below 350 K and observing the continuous formation of nanowires. We show the hysteresis in the order–disorder transition controlled by x-ray flux in the sample irradiated with continuous illumination. The shape of oxygen interstitial grains as they grow is anisotropic, showing Oi ordering under x-ray illumination in the *a*–*b* plane and in the *c*-axis direction.

(Some figures may appear in colour only in the online journal)

1. Introduction

In the last 25 years, quantum complex phenomena have been found in intrinsically heterogeneous bulks [1–3] and interfaces [4–6]. A heterogeneous phase of matter is a generic phenomenon, following doping of a highly correlated antiferromagnetic insulating electronic system. Recently, interstitial oxygen or oxygen vacancies have been shown to be a useful detail of the structure for the control of functionalities in complex oxides [7–10]. Therefore, the accumulated number of experimental data supports the existence of charge carriers segregated in different spatial domains (see figure 1) formed, for instance, by a self-organized superlattice of oxygen interstitials (Oi). The control of the grain size, along each of the three crystallographic directions, and of the lateral spatial segregation is of importance for tuning quantum size effects, which are known to be strongly dependent from the material architecture [11–13]. Controlling directly the architecture of the grains allows the manipulation of the sub-bands which actually are a function of the grain size. This is well established in film [14], where the enhancement or suppression of the superconducting critical temperature

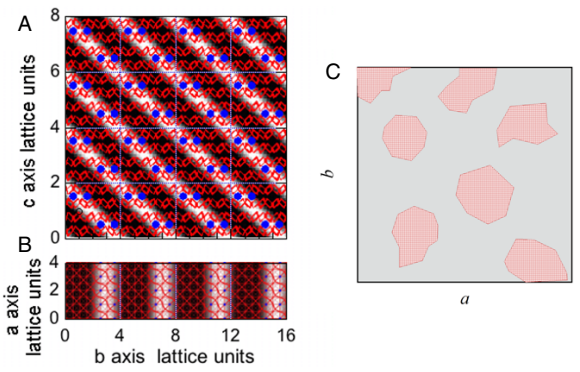

Figure 1. Ordered grains of Oi (blue dots) associated to the Q2 superstructure peaks in the *c*–*b* plane (A) and in the *a*–*b* plane (B) of the *Fmmm* crystal structure of La_2CuO_4. The red octahedra represent the CuO coordination units in the CuO_2 plane. (C) Schematic view of the spatial distribution of the ordered Oi grains (red polygons).

through a Fano resonance has long been proposed [15] and was later also proposed to be active in some more specific superlattices [16–18]. However, things become more complicated if we take account of recent data [8, 19] on the formation of a 'strange metal', arising because of the lateral self-organization of ordered defects, which are the origin of intricate network structures. There are, in fact, an increasing number of reports measuring the interplay among defects and superconductivity [20, 21], the role of defects in superfluidity [22], in quantum resonances [23] and phase transitions [24]. These data point out the essential role of heterogeneities for functionality as suggested by some authors in the early period of high temperature superconductivity [25, 26]. In fact, after the discovery of the K-doped FeSe superconductors, phase separation and iron vacancies have been immediately recognized [27–29]. Scanning tunneling microscopy (STM) has played a major role in this change of point of view in the last ten years both in colossal magnetoresistance [30] and high temperature superconducting materials [31–34]. On the other hand, STM focuses only on surface properties, and therefore it has not yet provided any clue for the relevance of bulk defects.

Bulk defects in high temperature superconductors have been investigated by synchrotron radiation scanning x-ray microdiffraction, which delivers on the sample x-ray beam with a spot size of one micron [35–37]. This technique has unveiled a complex pattern of Oi, associated to a specific reflection satellite called 'Q2', in the La_2CuO_{4+y} cuprate superconductor [7, 8]. Oxygen interstitials self-organize into fractal patterns, which establish spatial correlations connected with the measured T_c of the sample. As well as continuous x-ray irradiation of some manganites allowing the system to shift from an insulating to a metallic state [38], and in some organic amphiphile peptides from disorder to a spontaneous crystallization [39], it has been shown that continuous x-ray irradiation of the La_2CuO_{4+y} cuprate superconductor can be used to tune the system from a disordered pattern of Oi with a low T_c regime to a more ordered pattern of Oi, restoring a higher T_c [8]. This happens because Oi instead of becoming disordered in the crystal as a general consequence of the radiation damage, gets ordered as a function of the x-ray exposure time. Then, the annealing of the sample above the order–disorder transition temperature, $T_{Oi} = 330$ K, allows us to remove the Oi ordered complex pattern and to restore a low T_c state [8]. The connection between the ordering of dopant atoms like the out-of-plane oxygen interstitials and the charges in the CuO_2 planes is well verified for La_2CuO_{4+y}, but it has also been seen in other cuprates [40]. This connection has been used to describe the Oi ordering time evolution, assumed to occur together with the planar electronic phase separation [41]. Here we give a further description of the character of the order–disorder transition of oxygen interstitials, manipulating the sample by different temperatures and incident x-ray flux.

2. Materials and methods

Diffraction measurements on a single crystal of La_2CuO_{4+y} of size $3 \times 2 \times 0.5$ mm^3, were performed on the crystallography beamline, XRD1, at ELETTRA. The sample was grown first as La_2CuO_4 by the flux method and then doped by electrochemical oxidation. The x-ray beam, emitted by the wiggler source of a 2 GeV electron storage ring, was monochromatized by a Si(111) double crystal, and focused on the sample. The superconducting transitions of samples with different levels of average ordered Q2 volume have been established using contactless single-coil inductance. Our sample showed a sharp superconducting transition at T_c of about 37 K, as measured by surface resistivity in the radiofrequency region [7, 8]. The temperature of the crystal was monitored with an accuracy of ± 1 K. We have collected the data in the reflection geometry using a CCD detector, a photon energy of 12.4 keV (wavelength $\lambda =$ 1 Å) and a high x-ray flux reaching a maximum value of 1.6×10^{14} photons s^{-1} cm^{-2}. The beam size is of about 100 μm. We establish the photo-induced structural effects in the illuminated area by measuring the time evolution of the XRD pattern recorded by a CCD area detector. The CCD area detector records the x-ray reflections from the illuminated sample area and a surface layer of about 1.5 μm thickness. The striped Q2 domains are photo-switched in the same surface layer thickness of the sample. The sample oscillation around the *b* axis was in the range $0° < \Phi < 20°$, where Φ is the angle between the direction of the photon beam and the *a* axis. We have investigated a portion of the reciprocal space up to 0.6 Å^{-1} momentum transfer, i.e. recording the diffraction spots up to the maximum indices 3, 3, 19 in the a^*, b^*, c^* directions respectively. Thanks to the high brilliance source, it has been possible to record a large number of weak superstructure spots around the main peaks of the average structure. Twinning of the crystal has been taken into account to index the superstructure peaks. The orthorhombic lattice parameters of the single crystal were determined to be $a =$ (5.386 ± 0.004) Å, $b =$ (5.345 ± 0.008) Å, $c =$ (13.205 ± 0.031) Å at room temperature. The space group of the sample is *Fmmm*.

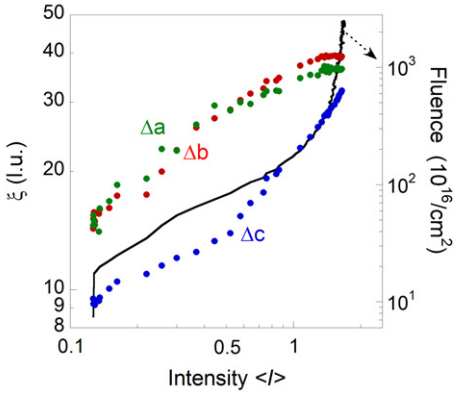

Figure 2. The evolution of size, ξ, at fixed temperature of 250 K of the Oi ordered domains along the a, b and c directions, Δa, Δb and Δc, as a function of the integrated intensity, $\langle I \rangle$, of the Q2 superstructure. The fluence, φ, as a function of $\langle I \rangle$ is also shown. The data used in this figure are from [7].

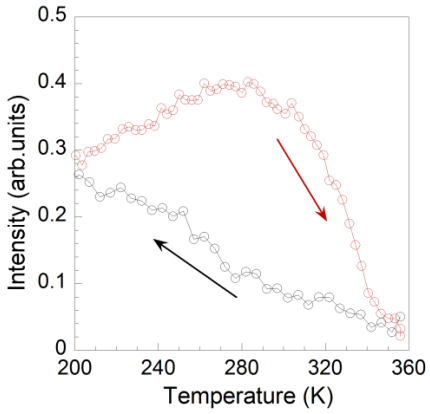

Figure 3. Integrated intensity of the q2 satellite reflections as a function of temperature measured using a beam with a low photon flux of 0.5×10^{14} photons cm^{-2} s^{-1}.

3. Results and discussion

The superstructure peak with wavevector $q2 = 0.09a^* + 0.25b^* + 0.5c^*$ is associated with the Oi ions arrangement in 3D ordered grains (see figures 1(A) and (B)); in particular, the Oi occupy the (1/4, 1/4, 1/4) site in the La_2O_{2+y} layers and pair to form stripes in the a direction with a period of four lattice units along the b axis in the a–b plane. Then, these stripes alternate in different layers with a c-axis periodicity of two lattice units. Figure 1(C) shows a pictorial scheme of the spatial distribution of the Oi ordered grains, whose size at room temperature is obtained from line peak analysis, being about 2.5 nm in the a-axis and b-axis directions, and 4 nm along the c-axis direction [7, 8].

The dynamics of Oi ordering has been studied by thermal cycle measurements, under continuous x-ray illumination. The sample has been prepared by removing the Q2 order by quenching the sample above $T_{Oi} = 330$ K, as shown elsewhere [7, 8]. Reporting measurements done in [7], surface resistivity in the radiofrequency region shows a superconducting transition at T_c of about 34, 35, 37, 38.5 and 40 K respectively if the Q2 intensity measured is 0.12, 0.6, 1.0, 1.1 and 1.2. Figure 2 shows therefore the evolution of the Oi unit cell grain size, ξ, under the effect of x-ray illumination at fixed temperature. FWHM^{-1} in reciprocal lattice units is ξ. The grain size has been measured using the standard procedure in x-ray diffraction from the broadening of the x-ray reflection lines in the k-space. For example, the size of a grain along the b crystallographic direction is calculated as $b/(\pi \times \text{FWHM})$. During the x-ray illumination, the size of Oi grains reaches the 45×45 unit cell size in the a–b plane, while it has an increase from 9 to about 30 lattice units in the c direction. However, the increase of lattice units in the c direction is mostly affected when the ordering in the a–b plane of the Oi grain size is around 25–30 unit cells. Then, we removed the Q2 order by quenching the sample again above $T_{Oi} = 330$ K and we started the next round of measurements at room temperature from a totally disordered Oi state. We collected the diffraction patterns at each temperature step at a rate of about 1.6×10^{-2} K s^{-1} and with a photon flux of $\phi_1 = 0.5 \times 10^{14}$ photons s^{-1} cm^{-2}, which is above the threshold required to trigger the Oi ordering process [7]. The thermal cycle was composed by a first heating ramp from 300 to 350 K; afterwards, a descending ramp down to 200 K was performed. Finally, heating up to room temperature allowed us to close the thermal cycle and restore the initial condition of Oi order. Figure 3 shows a large hysteresis as a result of this first experiment, suggesting a continuous phase transition between an ordered and disordered phase. Indeed, visual inspection of the loop does not show any sharp jump between the ordered and the disordered phases of Oi, but rather a smooth transition, with the presence, along the curve, of tiny jumps. There is the formation of small local domains in local regions—called *avalanches*—that move from the ordered phase to the disordered one. Each small domain transforms independently to a smooth, not sharp, hysteresis at the macroscopic level. By adding disorder (or an external field) until the critical value, the system is subjected to catastrophic events, showing a power law distribution [42–45] as revealed by micro-x-ray diffraction and continuous x-ray illumination investigations [7, 8]. This reveals a delicate balance between disorder, interactions, and material anisotropy. In some cuprate superconductors, in fact, analysis of the data extracted from STM shows that the electron nematic is fractal in nature and that it extends throughout the bulk of the material [46].

Figures 4(A) and (B) show the coherence length, ξ, as a function of temperature along the b and c directions respectively. The anisotropic feature of the order–disorder transition is shown by the different behaviour of the size of the ordered domains, along the different crystallographic directions. Indeed, the ordering in the early stage occurs first in the a–b plane, involving about 15×15 lattice units in a and b directions, while few cells, about three, are interested in the c direction. During the cooling, the size of Oi grains reaches the 40×40 unit cell size in the a–b plane, while it has a slight increase from 4 to about 7 lattice units in the c direction. Then, in the subsequent heating ramp, the ordering appears to be favoured in the c direction; in fact, we pass from

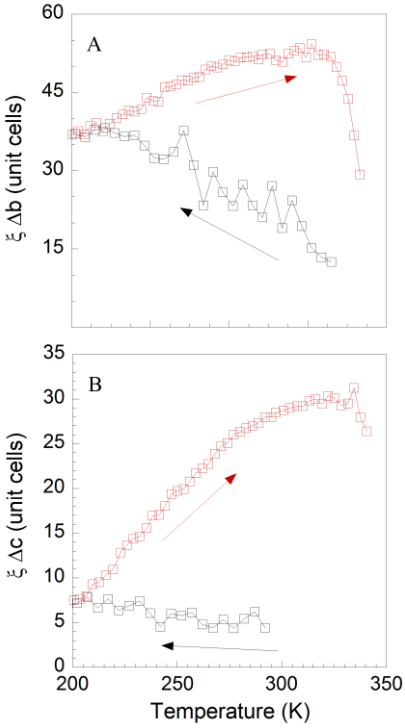

Figure 4. The coherence length, ξ, along b (A) and c (B) measured at low flux $\Phi = 0.5 \times 10^{14}$ photons cm^{-2} s^{-1} during the thermal cycle. Cooling and heating processes are indicated by black and red squares respectively.

45×45 to 50×50 lattice units in the a–b plane, and from 7 to 35 lattice units in the c direction. The character of the transition is smooth and therefore these results point towards a continuous nature of the Oi order–disorder phase transition. In fact, phase transitions in scalar field theory indicate that the strength of the transition is not a minor quantitative detail of the transition, but of considerable impact concerning the phase conversion mechanism [47–49].

Figure 5 shows a hysteresis as a result of a second experiment in which the same thermal cycle was performed, illuminating the sample with higher x-ray flux of $\phi_1 = 5 \times 10^{14}$. In this case the resulting hysteresis curve was narrow in comparison to that shown in figure 3, and thus typical of a first-order phase transition. The higher x-ray photon flux increases the dynamic of the Oi and speeds up the ordering process, lifting the tiny jumps of the phase conversion mechanism. As a consequence, the hysteresis is closed at a temperature exceeding about 100 K figure 3.

Figures 6(A) and (B) show the coherence length, ξ, as a function of temperature along the b and c directions respectively. The features of the order-to-disorder transition are given now by the sharp increasing and decreasing of ξ, at $T = 305$ K during the cooling and $T = 335$ K during the heating. This means the presence of two *jumps* in the size of the ordered domains both in the a–b plane and along the c direction, during the thermal cycle. The minimum and maximum size values are the same found in the first experiment; but, in this case, what is quite different is the discontinuous character of size change. Indeed, we pass from

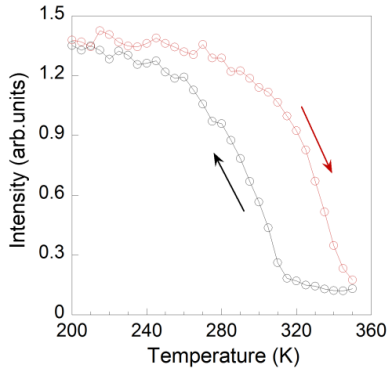

Figure 5. Integrated intensity of the q2 satellite reflections as a function of temperature measured using a beam with a high photon flux of 5×10^{14} photons cm^{-2} s^{-1}. The higher flux results in a narrowing of the curve.

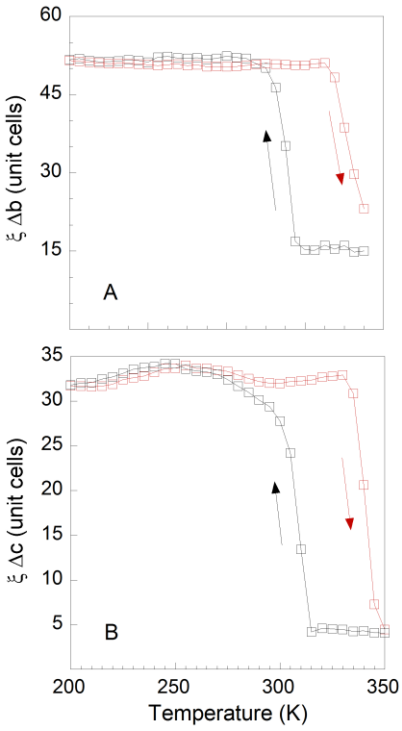

Figure 6. The coherence length, ξ, along b and c measured with $\Phi = 5 \times 10^{14}$ photons cm^{-2} s^{-1} as a function of temperature, during the cooling process (black square) and the heating process (red square).

minimum to maximum size in a few kelvin, both in the cooling and in the heating ramp, confirming the behaviour of a typical first-order phase transition.

4. Conclusions

We have shown a new set of experiments probing the evolution of Oi grain size and phase segregation by thermal treatments and x-ray continuous illumination, providing a new experimental avenue for tuning the grain size of the system. The hysteresis of the Oi ordering has been shown for two

different levels of x-ray flux irradiation of the sample. The hysteresis width decreases with the increasing of the incident photon flux, indicating that the photon flux increases the ordering dynamics. The disorder–order transition of the Oi is tuned from a weak first-order–disorder phase transition towards an ordinary discontinuous first-order phase transition by increasing the photon flux of the continuous x-ray illumination. The present findings confirm the self-organized nature of the oxygen interstitial ions in La_2CuO_{4+y} and could be of inspiration for the design of rewritable superconducting devices in intrinsically disordered materials which show a high ionic conductivity as well [50]. In fact, in a specific range of temperature, thermal treatments remove the ion ordering (oxygen interstitials) and x-ray continuous illumination could be used as an efficient tool to restore the required and functional level of ordering in the material.

References

[1] Bednorz J G and Müller K A 1988 Perovskite-type oxides-the new approach to high-T_c superconductivity *Rev. Mod. Phys.* **60** 585–600

[2] Dagotto E 2005 Complexity in strongly correlated electronic systems *Science* **309** 257–62

[3] Ioffe L B and Gershenson M E 2012 Quantum phase transitions: emergent inhomogeneity *Nature Mater.* **11** 567–8

[4] Hwang H Y, Iwasa Y, Kawasaki M, Keimer B, Nagaosa N and Tokura Y 2012 Emergent phenomena at oxide interfaces *Nature Mater.* **11** 103–13

[5] Brinkman A, Huijben M, van Zalk M, Huijben J, Zeitler U, Maan J C, van der Wiel W G, Rijnders G, Blank D H A and Hilgenkamp H 2007 Magnetic effects at the interface between non-magnetic oxides *Nature Mater.* **6** 493–6

[6] Huijben M, Rijnders G, Blank D H A, Bals S, Aert S V, Verbeeck J, Tendeloo G V, Brinkman A and Hilgenkamp H 2006 Electronically coupled complementary interfaces between perovskite band insulators *Nature Mater.* **5** 556–60

[7] Poccia N, Fratini M, Ricci A, Campi G, Barba L, Vittorini-Orgeas A, Bianconi G, Aeppli G and Bianconi A 2011 Evolution and control of oxygen order in a cuprate superconductor *Nature Mater.* **10** 733–6

[8] Fratini M, Poccia N, Ricci A, Campi G, Burghammer M, Aeppli G and Bianconi A 2010 Scale-free structural organization of oxygen interstitials in La_2CuO_{4+y} *Nature* **466** 841–4

[9] Zaanen J 2010 High-temperature superconductivity: the benefit of fractal dirt *Nature* **466** 825–7

[10] Littlewood P 2011 Superconductivity: an x-ray oxygen regulator *Nature Mater.* **10** 726–7

[11] Bianconi G 2012 Superconductor-insulator transition on annealed complex networks *Phys. Rev.* E **85** 061113

[12] Bianconi A, Saini N L, Agrestini S, Di Castro D and Bianconi G 2000 The strain quantum critical point for superstripes in the phase diagram of all cuprate perovskites *Int. J. Mod. Phys.* B **14** 3342–55
Bianconi A, Agrestini S, Bianconi G, Di Castro D and Saini N L 2001 A quantum phase transition driven by the electron lattice interaction gives high T_c superconductivity *J. Alloys Compounds* **317** 537–41

[13] Araújo M A N, García-García A M and Sacramento P D 2011 Enhancement of the critical temperature in iron-pnictide superconductors by finite size effects *Phys. Rev.* B **84** 172502
Brihuega I, García García A M, Ribeiro P, Ugeda M M, Michaelis C H, Bose S and Kern K 2011 Experimental observation of thermal fluctuations in single superconducting Pb nanoparticles through tunneling measurements *Phys. Rev.* B **84** 104525

[14] Shanenko A A, Croitoru M D and Peeters F M 2006 Quantum-size effects on T_c in superconducting nanofilms *Europhys. Lett.* **76** 498

[15] Blatt J M and Thompson C J 1963 Shape resonances in superconducting thin films *Phys. Rev. Lett.* **10** 332

[16] Perali A, Bianconi A, Lanzara A and Saini N L 1996 The gap amplification at a shape resonance in a superlattice of quantum stripes: a mechanism for high T_c *Solid State Commun.* **100** 181–6

[17] Bianconi A, Valletta A, Perali A and Saini N L 1997 High T_c superconductivity in a superlattice of quantum stripes *Solid State Commun.* **102** 369–74

[18] Innocenti D, Poccia N, Ricci A, Valletta A, Caprara S, Perali A and Bianconi A 2010 Resonant and crossover phenomena in a multiband superconductor: tuning the chemical potential near a band edge *Phys. Rev.* B **82** 184528

[19] Poccia N, Ricci A and Bianconi A 2011 Fractal structure favoring superconductivity at high temperatures in a stack of membranes near a strain quantum critical point *J. Supercond. Novel Magn.* **24** 1195–200

[20] Alloul H, Bobroff J, Gabay M and Hirschfeld P J 2009 Defects in correlated metals and superconductors *Rev. Mod. Phys.* **81** 45–108

[21] Geballe T H and Marezio M 2009 Enhanced superconductivity in Sr_2CuO_{4-y} *Physica* C **469** 68

[22] Pollet L, Boninsegni M, Kuklov A, Prokof'ev N, Svistunov B and Troyer M 2010 The role of defects in supersolid helium-4 *Phys. Proc.* **7** 80–4

[23] Chen J-H, Li L, Cullen W G, Williams E D and Fuhrer M S 2011 Tunable Kondo effect in graphene with defects *Nature Phys.* **7** 535

[24] Richardella A, Roushan P, Mack S, Zhou B, Huse D A, Awschalom D D and Yazdani A 2010 Visualizing critical correlations near the metal–insulator transition in $Ga_{1-x}Mn_xAs$ *Science* **327** 665–9

[25] Gor'kov L P and Teitel'baum G B 2008 The two-component physics in cuprates in the real space and in the momentum representation *J. Phys.: Conf. Ser.* **108** 012009

[26] Müller K A and Bussmann-Holder A (ed) 2005 *Superconductivity in Complex Systems* (*Structure and Bonding* vol 114) (Berlin: Springer)

[27] Ricci A *et al* 2011 Nanoscale phase separation in the iron chalcogenide superconductor $K_{0.8}Fe_{1.6}Se_2$ as seen via scanning nanofocused x-ray diffraction *Phys. Rev.* B **84** 060511

[28] Li W *et al* 2011 Phase separation and magnetic order in *k*-doped iron selenide superconductor *Nature Phys.* **8** 126–30

[29] Ksenofontov V, Wortmann G, Medvedev S A, Tsurkan V, Deisenhofer J, Loidl A and Felser C 2011 Phase separation in superconducting and antiferromagnetic $K_{0.8}Fe_{1.6}Se_2$ by Mössbauer spectroscopy *Phys. Rev.* B **84** 180508

[30] Renner B B, Tokunaga C, Tokura Y and Aeppli G 2011 Imaging oxygen defects and their motion at a manganite surface *Nature Commun.* **2** 212

[31] McElroy K, Lee J, Slezak J A, Lee D H, Eisaki H, Uchida S and Davis J C 2005 Atomic-scale sources and mechanism of nanoscale electronic disorder in $Bi_2Sr_2CaCu_2O_{8+\delta}$ *Science* **309** 1048–52

[32] Slezak J A, Lee J, Wang M, McElroy K, Fujita K, Andersen B M, Hirschfeld P J, Eisaki H, Uchida S and Davis J C 2008 Imaging the impact on cuprate superconductivity of varying the interatomic distances within individual crystal unit cells *Proc. Natl Acad. Sci.* **105** 3203–8

[33] Wise W D *et al* 2009 Imaging nanoscale fermi-surface variations in an inhomogeneous superconductor *Nature Phys.* **5** 213–6
[34] Mesaros A, Fujita K, Eisaki H, Uchida S, Davis J C, Sachdev S, Zaanen J, Lawler M J and Kim E-A 2011 Topological defects coupling smectic modulations to intra-unit-cell nematicity in cuprates *Science* **333** 426–30
[35] Ice G E, Budai J D and Pang J W L 2011 The race to x-ray microbeam and nanobeam science *Science* **334** 1234–9
[36] Poccia N, Campi G, Fratini M, Ricci A, Saini N L and Bianconi A 2011 Spatial inhomogeneity and planar symmetry breaking of the lattice incommensurate supermodulation in the high-temperature superconductor $Bi_2Sr_2CaCu_2O_{8+y}$ *Phys. Rev.* B **84** 100504
[37] Agrestini S, Saini N L, Bianconi G and Bianconi A 2003 The strain of CuO_2 lattice: the second variable for the phase diagram of cuprate perovskites *J. Phys. A: Math. Gen.* **36** 9133–42
[38] Kiryukhin V, Casa D, Hill J P, Keimer B, Vigliante A, Tomioka Y and Tokura Y 1997 An x-ray-induced insulator–metal transition in a magnetoresistive manganite *Nature* **386** 813–5
[39] Cui H, Pashuck E T, Velichko Y S, Weigand S J, Cheetham A G, Newcomb C J and Stupp S I 2010 Spontaneous and x-ray-triggered crystallization at long range in self-assembling filament networks *Science* **327** 555–9
[40] Ofer R and Keren A 2009 Nutation versus angular-dependent NQR spectroscopy and impact of underdoping on charge inhomogeneities in $YBa_2Cu_3O_y$ *Phys. Rev.* B **80** 224521
[41] de Mello E V L 2012 Description and connection between the oxygen order evolution and the superconducting transition in La_2CuO_{4+y} *Europhys. Lett.* **98** 57008
[42] Sethna J P, Dahmen K, Kartha S, Krumhansl J A, Roberts B W and Shore J D 1993 Hysteresis and hierarchies: dynamics of disorder-driven first-order phase transformations *Phys. Rev. Lett.* **70** 3347–50
[43] Dahmen K and Sethna J P 1996 Hysteresis, avalanches, and disorder-induced critical scaling: a renormalization-group approach *Phys. Rev.* B **53** 14872–905
[44] Perković O, Dahmen K A and Sethna J P 1999 Disorder-induced critical phenomena in hysteresis: numerical scaling in three and higher dimensions *Phys. Rev.* B **59** 6106–19
[45] Sethna J P, Dahmen K A and Myers C R 2001 Crackling noise *Nature* **410** 242–50
[46] Phillabaum B, Carlson E W and Dahmen K A 2012 Spatial complexity due to bulk electronic nematicity in a superconducting underdoped cuprate *Nature Commun.* **3** 915
[47] Littlewood P B and Chandra P 1986 Delayed nucleation at a weakly first-order transition *Phys. Rev. Lett.* **57** 2415–8
[48] Aizenman M and Wehr J 1989 Rounding of first-order phase transitions in systems with quenched disorder *Phys. Rev. Lett.* **62** 2503–6
[49] Berges J, Tetradis N and Wetterich C 1997 Coarse graining and first order phase transitions *Phys. Lett.* B **393** 387–94
[50] Dyre J C, Maass P, Roling B and Sidebottom D L 2009 Fundamental questions relating to ion conduction in disordered solids *Rep. Prog. Phys.* **72** 046501